Article

Immunity

The Nlrp3 Inflammasome Suppresses Colorectal Cancer Metastatic Growth in the Liver by Promoting Natural Killer Cell Tumoricidal Activity

Graphical Abstract

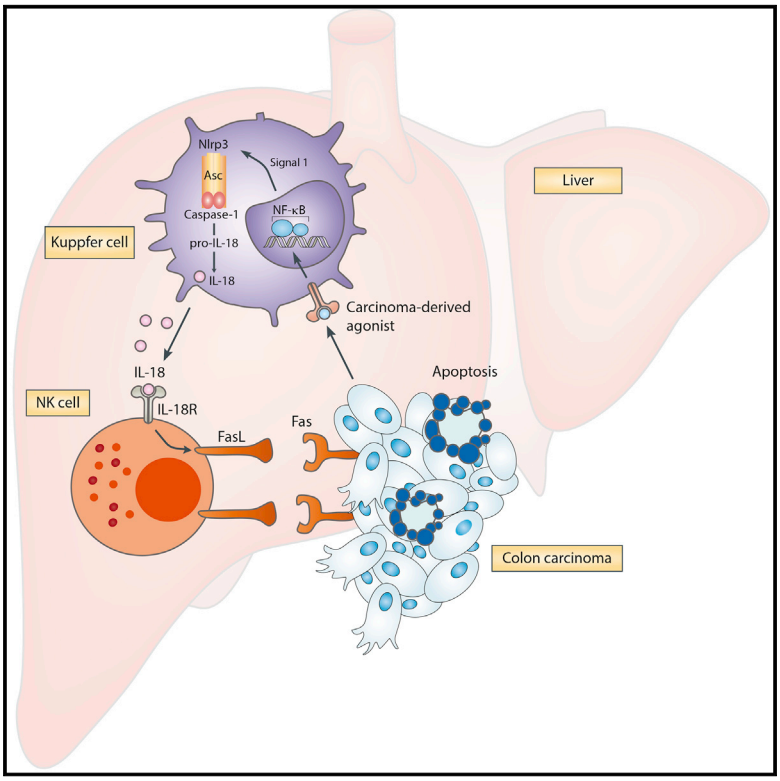

Authors

Jeremy Dupaul-Chicoine, Azadeh Arabzadeh, Maryse Dagenais, ..., Sara L. Colpitts, Nicole Beauchemin, Maya Saleh

Correspondence

maya.saleh@mcgill.ca

In Brief

Although the role of adaptive immunity in cancer immunosurveillance is established, that of innate immunity is not. Saleh and colleagues define a regulatory circuitry within the innate immune system that links inflammasome stimulation by cancer-associated agonists to activation of NK cell tumoricidal function leading to tumor elimination at metastatic sites.

Highlights

- The Nlrp3 inflammasome suppresses liver colon cancer metastatic growth
- Inflammasome-induced immunosurveillance requires NK cells but not T and B cells
- IL-18, but not IL-1β, mediates NK cell maturation and tumoricidal activity
- IL-18 licenses tumor killing by NK cells independent of IFN-γ

Dupaul-Chicoine et al., 2015, Immunity *43*, 751–763
October 20, 2015
http://dx.doi.org/10.1016/j.immuni.2015.08.013

Immunity
Article

The Nlrp3 Inflammasome Suppresses Colorectal Cancer Metastatic Growth in the Liver by Promoting Natural Killer Cell Tumoricidal Activity

Jeremy Dupaul-Chicoine,[1] Azadeh Arabzadeh,[2] Maryse Dagenais,[1] Todd Douglas,[3] Claudia Champagne,[4] Alexandre Morizot,[4] Ian Gaël Rodrigue-Gervais,[4] Valérie Breton,[2] Sara L. Colpitts,[5] Nicole Beauchemin,[1,2,4] and Maya Saleh[1,2,3,4,*]

[1]Department of Biochemistry, McGill University, Montréal, QC H3G 1Y6, Canada
[2]The Goodman Cancer Research Centre, McGill University, Montréal, QC H3A 1A3, Canada
[3]Department of Microbiology and Immunology, McGill University, Montréal, QC H3A 2B4, Canada
[4]Department of Medicine, McGill University, Montréal, QC H3G 0B1, Canada
[5]Department of Immunology, Center for Integrated Immunology and Vaccine Research, UConn Health, Farmington, CT 06030, USA
*Correspondence: maya.saleh@mcgill.ca
http://dx.doi.org/10.1016/j.immuni.2015.08.013

SUMMARY

The crosstalk between inflammation and tumorigenesis is now clearly established. However, how inflammation is elicited in the metastatic environment and the corresponding contribution of innate immunity pathways in suppressing tumor growth at secondary sites are poorly understood. Here, we show that mice deficient in Nlrp3 inflammasome components had exacerbated liver colorectal cancer metastatic growth, which was mediated by impaired inteleukin-18 (IL-18) signaling. Control of tumor growth was independent of differential cancer cell colonization or proliferation, intestinal microbiota effects, or tumoricidal activity by the adaptive immune system. Instead, the inflammasome-IL-18 pathway impacted maturation of hepatic NK cells, surface expression of the death ligand FasL, and capacity to kill FasL-sensitive tumors. Our results define a regulatory signaling circuit within the innate immune system linking inflammasome activation to effective NK-cell-mediated tumor attack required to suppress colorectal cancer growth in the liver.

INTRODUCTION

Colorectal cancer (CRC) is the third most commonly diagnosed cancer globally, accounting for an annual 1.36 million cancer cases and 694,000 deaths in the US (Ferlay et al., 2015). The prognosis of CRC patients is good for early-stage cancer, but the majority of cases are diagnosed at later stages. It is estimated that approximately 40% of CRC patients progress to fatal metastasis (Tsikitis et al., 2014), 80% being confined to the liver while the remaining 20% are associated with other visceral organs (Manfredi et al., 2006).

Inflammation and immunity are important determinants of tumorigenesis, impacting cancer development from initiation, promotion, and progression to cancer equilibrium and suppression, respectively (Balkwill and Coussens, 2004; Schreiber et al., 2011). Although cell-autonomous aberrations are considered the initiators of cancer, the interaction of cancer cells with their microenvironment, particularly with immune cells therein, results in stimulatory or inhibitory effects that govern tumor escape versus elimination. Although much effort has been invested in deciphering the function of the adaptive immune system in tumor immunosurveillance (Galon et al., 2013; Schreiber et al., 2011), the contribution of specific innate immunity pathways to this process is less understood. Among the effectors of the innate immune system are germline-encoded pattern recognition receptors (PRRs) that, upon sensing microbial- or danger-associated molecular patterns, elicit an inflammatory response to restore homeostasis. A number of PRRs, including members of the Nod-like receptor (NLR) and HIN200 families, operate by assembling large molecular complexes referred to as inflammasomes (Latz et al., 2013). These signaling scaffolds trigger innate immunity by activating the protease caspase-1, which cleaves immune and metabolic substrates (Keller et al., 2008; LeBlanc et al., 2014; Shao et al., 2007), most notably the pro-inflammatory cytokines interleukin-1β (IL-1β) and IL-18, inducing inflammation and an inflammatory form of cell death termed pyroptosis (Labbé and Saleh, 2008).

We and others have previously implicated the inflammasome pathway in suppression of colitis and colitis-associated colorectal cancer. Mice deficient in inflammasome components, including Nlrp3, Nlrp6, Asc, caspase-1 and caspase-11, Il-18 or Il-18r, exhibit increased colitis and tumorigenesis compared to wild-type (WT) mice in the azoxymethane-dextran sulfate sodium (AOM-DSS) model (Allen et al., 2010; Dupaul-Chicoine et al., 2010; Elinav et al., 2011; Huber et al., 2012; Salcedo et al., 2010; Zaki et al., 2010a, 2010b). The tumor-suppressive effect of the inflammasome in this context was not at the level of immunosurveillance but mediated by the function of IL-18 in maintaining epithelial barrier integrity and triggering tissue repair after ulceration.

IL-1β and IL-18 exert pleiotropic effects in inflammation and tumorigenesis. Indeed, both pro- and anti-tumorigenic functions have been previously reported for these cytokines. For instance,

IL-1β is spontaneously produced by advanced melanomas, conferring growth advantage and invasion (Okamoto et al., 2010; Qin et al., 2011). Transgenic expression of human *IL1B* in the stomach of mice also promotes tumorigenesis through autocrine effects on NF-κB activation and recruitment of myeloid-derived suppressor cells (MDSCs) (Tu et al., 2008). In contrast, IL-1β is necessary for anti-cancer immunosurveillance after chemotherapy (Eisenbarth and Flavell, 2009; Ghiringhelli et al., 2009). Similarly to IL-1β, IL-18 performs dual functions in tumorigenesis. Besides its indirect tumor-suppressive role in colitis-associated CRC, IL-18 has been classically associated with a T helper 1 skewed immunostimulatory anti-tumorigenic response through its ability to induce IFN-γ (Okamura et al., 1995) and its effects on enhancing the cytolytic activity of T cells and NK cells (Novick et al., 2013). In contrast to these anti-tumorigenic functions, IL-18 enhances, rather than suppresses, hepatic melanoma metastasis. Carrascal et al. (2003) demonstrated that IL-18 signaling stimulated microvascular arrest of tumor cells through modulation of endothelial cell adhesion. Furthermore, a more recent study reported an inhibitory effect of IL-18 on NK cell tumoricidal function through induction of the immunosuppressive co-stimulatory molecule PD-1 on their surface (Terme et al., 2011).

The seemingly contradictory function of inflammasome-dependent cytokines in tumor promotion and anti-tumor immunity is proposed to be context dependent and tissue specific. Because the tumors in most spontaneous and experimental CRC animal models do not progress to metastases, and because the primary site of CRC metastasis is the liver, an immunologically unique organ with a relatively tolerogenic microenvironment (Jenne and Kubes, 2013), we chose to use an intrasplenic model of CRC metastasis to the liver to genetically dissect the impact of the inflammasome pathway on the immune surveillance mechanisms of syngenic metastatic lesions in vivo. We demonstrate a critical role for the Nlrp3 inflammasome in suppressing CRC growth in the liver. IL-18, but not IL-1 signaling, was required for inflammasome-mediated immunosurveillance. Both the production and the response to this cytokine relied solely on the innate immune system. IL-18 controlled metastatic growth, independently of T and B cells, by promoting hepatic NK cell maturation and priming Fas-mediated cytotoxicity. The anti-tumorigenic function of the inflammasome required Fas-sensitive tumors and could be recapitulated in an independent model of lung metastasis. This study defines a regulatory circuitry in the innate immune system that links inflammasome activation by endogenous danger signals to efficient activation of NK cell tumoricidal function leading to tumor elimination at metastatic sites.

RESULTS

Caspase-1-Deficient Mice Are Highly Susceptible to Colorectal Cancer Liver Metastatic Growth

To investigate the role of the inflammasome in liver CRC metastasis, we implemented a model of intrasplenic injection of transplantable tumor cells derived from a murine primary colon carcinoma (MC38) (Rosenberg et al., 1986) that lead to liver metastasis in a C57BL/6 syngenic immunocompetent host. Because caspase-1 is the central effector of all canonical inflammasomes defined to date, we first evaluated the metastatic burden of caspase-1-deficient mice (also carrying an inactivating mutation in *Casp-11*; herein referred to as *Ice*$^{-/-}$ mice) compared to that of C57BL/6 WT mice on days 14 and 21 post-injection (p.i.) (Figure 1A). Until day 14 p.i., the weight of the liver did not vary from that of untreated mice and was similar between WT and *Ice*$^{-/-}$ mice (Figures 1B, 1D, and S1A). Quantification of MC38 foci coverage (herein denoted as "metastatic foci") on hematoxylin and eosin (H&E)-stained liver tissue sections revealed a similar area covered by metastatic lesions on day 14 p.i. between the two mouse genotypes (Figures 1B and 1E). In contrast, we observed that *Ice*$^{-/-}$ mice had heavier livers compared to WT animals starting on day 18 p.i. (Figure S1A), and this difference was more marked on day 21 p.i. (Figures 1C and 1F). Histological analysis revealed that changes in liver weight correlated with larger hepatic MC38 foci coverage in *Ice*$^{-/-}$ mice compared to WT animals (Figures 1C and 1G). To address the basis of this differential tumor growth, we first determined whether ablation of inflammasome signaling might have resulted in a pre-damaged liver at baseline. Quantification of the two liver enzymes AST and ALT in the circulation revealed no differences in liver damage between WT and *Ice*$^{-/-}$ mice (Figure S1B). Next, we evaluated whether cancer cell proliferation or cell death were affected by loss of inflammasome signaling. We assessed cell proliferation potential in metastatic foci on days 14 and 21 p.i. by immunofluorescence staining of liver tissue sections with antibodies against proliferating cellular nuclear antigen (PCNA). Histological examination (Figure 1H) and quantification (Figure 1I) of PCNA^{+} cells revealed no differences in proliferation between WT and *Ice*$^{-/-}$ mice. In contrast, TUNEL staining that marks dying cells revealed reduced cell death levels in metastatic foci in *Ice*$^{-/-}$ mice compared to WT mice at equivalent tumor burden on day 14 p.i. (Figures 1J and 1K). Co-staining of liver sections with TUNEL and antibodies against cytokeratin 20 that labels intestinal epithelial cells (IECs) indicated that cell death occurred primarily in the MC38 colorectal cancer cells (Figure 1L). Together, these results suggest that activation of the inflammatory caspase pathway suppresses MC38 growth in the liver by triggering cell death of colon carcinoma cells within metastatic foci.

Nlrp3, but Not Nlrc4 or Aim2, Is Required for Suppression of CRC Metastatic Growth in the Liver

Caspase-1 is synthesized as a zymogen, which requires activation by proximity within an inflammasome for biological activity. Seven inflammasomes have been defined to date, each responding to distinct sets of stimuli. NLRP3 recognizes a wide array of cellular stress signals, including ionic disturbances, metabolites, mitochondrial stress, high extracellular ATP concentrations, particulate matters, and microbial products (Latz et al., 2013). In contrast, NLRC4 and AIM2 are restricted to sensing bacterial flagellum components and cytosolic DNA, respectively (Latz et al., 2013). Because the liver is continuously exposed to diverse microbial products through the portal vein circulation, and because danger-associated molecular patterns (DAMPs) are likely to be released in the metastatic environment, we examined the role of different inflammasome-forming NLR proteins and AIM2 in the control of CRC metastatic growth. In contrast to *Ice*$^{-/-}$ mice, both *Nlrc4*$^{-/-}$ mice and *Aim2*$^{-/-}$ mice had an unadulterated tumor control mechanism, exhibiting no differences in either

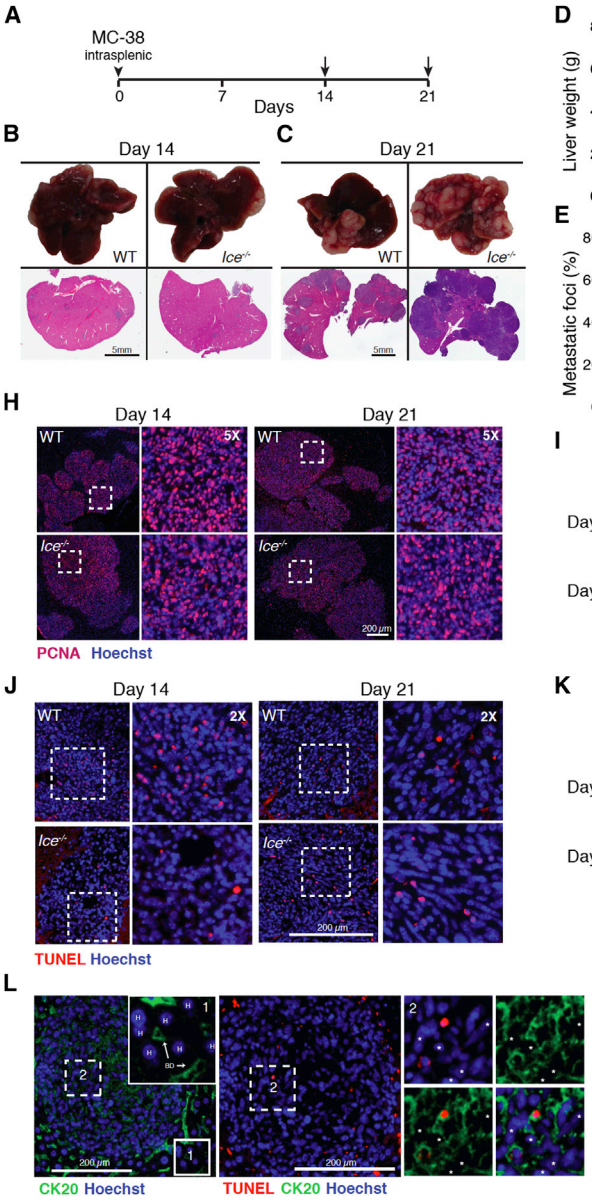

Figure 1. *Ice*$^{-/-}$ Mice Exhibit Enhanced MC38 Colorectal Cancer Growth in the Liver

(A) Schematic representation of CRC metastatic growth in the liver model induced by intrasplenic injection of the C57BL/6 colon carcinoma MC38 cells. Mice were injected on day 0 and sacrificed on either day 14 or 21 post-injection.

(B and C) Representative pictures of the liver and hematoxylin and eosin (H&E) staining of liver sections from WT and *Ice*$^{-/-}$ mice sacrificed on day 14 (B) or 21 (C) after MC38 intrasplenic injection.

(D–G) WT or *Ice*$^{-/-}$ mice liver weight (D and F) and CRC foci coverage (E and G) on day 14 (D and E) or 21 (F and G) after MC38 injection ($n \geq 4$ per time point per genotype).

(H–K) Epifluorescence images of MC38 foci in liver sections from WT or *Ice*$^{-/-}$ mice on day 14 or 21 post-MC38 injection stained with antibodies against PCNA to mark dividing cells (H) or TUNEL to mark dying cells (J) and Hoechst to label nuclei. Insets correspond to boxed regions. n = 3 mice per genotype. Scale bars represent 200 μm. Quantification of stain-positive cells in (H) and (J) shown in (I) and (K), respectively.

(L) Immunofluorescence images of MC38 foci in liver sections stained with TUNEL and antibodies against cytokeratin 20 (CK20) that mark intestinal epithelial cells and bile duct (BD) cells but not hepatocytes (H) (scale bars represent 200 μm); inset 1, zoom 2.5×; inset 2, zoom 2×. Asterisks label CK20-negative cells that are also TUNEL negative.

Graphs represent the mean ± SEM. Statistical analysis was performed with Student's t test; *$p < 0.05$, **$p < 0.001$, ***$p < 0.0001$. All experiments were repeated two to three times. See also Figure S1.

liver weight or metastatic coverage compared to WT animals on day 21 p.i. (Figures 2A–2D). *Nlrp3*$^{-/-}$ mice phenocopied *Ice*$^{-/-}$ mice, showing higher tumor burden in the liver, as measured by liver weight (Figure 2E) and foci coverage (Figure 2F). Nlrp3 inflammasome activation is tightly regulated and requires two signals for activation: a priming signal (or signal 1) that generally converges on NF-κB activation and is needed to induce Nlrp3 expression, and an activating signal (or signal 2) required for complex assembly (Latz et al., 2013). To determine whether the MC38 adenocarcinoma cells released factors that primed or activated Nlrp3, we examined the effect of MC38 conditioned media (CM) on the inflammasome response by using bone-marrow-derived macrophages (BMDMs). MC38-derived CM, but not control CM from BMDMs, robustly primed the inflammasome response, inducing caspase-1 activation and secretion of IL-1β and IL-18 when combined with a signal 2 (e.g., ATP) (Figures 2G, 2H, and S2A). To decipher inflammasome-activating signals in the tumor microenvironment in vivo, we first assessed the contribution of the microbiota. We administered an antibiotic cocktail in the drinking water of WT mice from the time of weaning until sacrifice for a total duration of 9 weeks (Figure 2I). Quantification of bacterial 16S rRNA in the mouse fecal pellets by qPCR showed a marked depletion of the microbiota between untreated and treated mice (~4-log difference) (Figure S2B). However, this microbiota deregulation did not impact tumor growth, as shown by the fact that liver weight was equivalent in the two groups (Figure 2J). Next, we pharmacologically assessed the contribution of three potential DAMPs, namely reactive oxygen species (ROS), uric acid, and extracellular ATP (Latz et al., 2013). We treated MC38-bearing WT mice with N-acetylcysteine (NAC) to quench ROS, allopurinol to block the production of uric acid, or suramin to inhibit P2 receptors, including extracellular ATP signaling (Figure 2I). Although NAC or allopurinol administration did not impact liver weight or MC38 foci coverage (Figures 2K and 2L), treatment with suramin resulted in increased tumor burden in the liver (Figures 2M and 2N). Nlrp3 activation downstream of extracellular ATP signaling has previously been demonstrated in the context

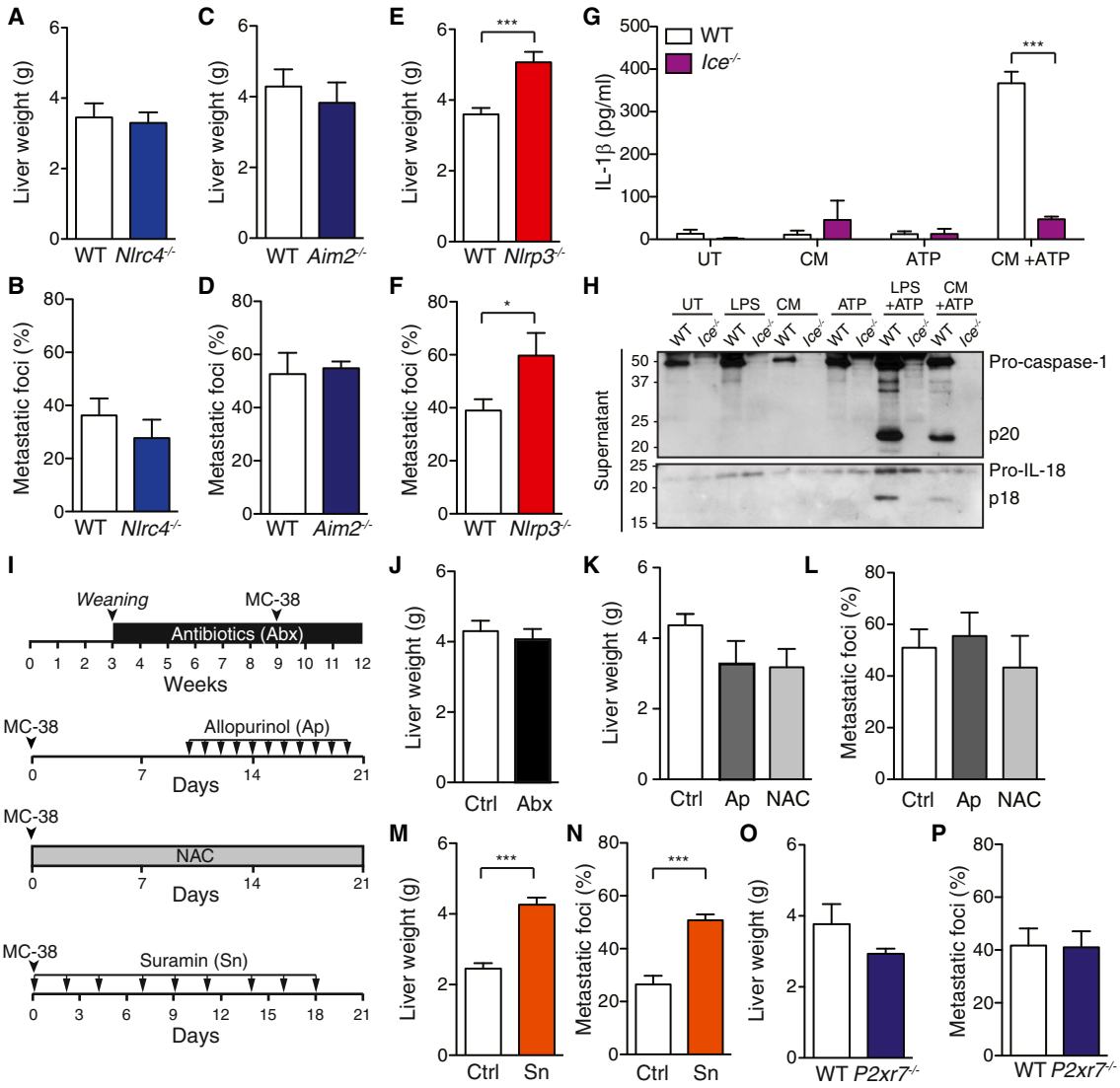

Figure 2. The NLRP3 Inflammasome Is Required for Suppression of MC38 Growth in the Liver Independently of P2x7r

(A–F) *Nlrc4*$^{-/-}$ mice (A, B), *Aim2*$^{-/-}$ mice (C, D), or *Nlrp3*$^{-/-}$ mice (E, F) liver weight (A, C, E) and metastatic foci coverage (B, D, F) compared to WT mice on day 21 after intrasplenic injection of MC38 cells (n $\geq$ 4 mice per genotype per experiment).

(G) ELISA quantification of IL-1β levels in BMDMs from either WT (n = 5) or *Ice*$^{-/-}$ (n = 3) mice. BMDMs were left untreated (UT) or treated with MC38 conditioned media (CM), ATP, or CM+ATP.

(H) Immunoblot analysis of caspase-1 and IL-18 levels in the supernatant of BMDMs from (G).

(I) Schematic representation of the antibiotic, allopurinol (Ap), NAC, or suramin (Sn) treatment regimens. At weaning (week 3), WT mice were administered an antibiotic cocktail (Abx) in their drinking water for 9 weeks. WT mice were injected with allopurinol (10 mg/g) i.p. from day 10 to day 20. 1% NAC was added to the drinking water of WT mice throughout the experiment. WT mice were injected i.p. with either PBS or suramin (1 mg) in 100 μl PBS starting on day 0, three times per week until the end of the experiment.

(J) Liver weight of control (Ctrl, regular water) or Abx-treated WT mice 21 days after intrasplenic MC38 injection (n = 10 mice per treatment).

(K and L) Liver weight (K) and CRC foci coverage (L) of control (Ctrl), allopurinol (Ap), or NAC-treated WT mice 21 days after intrasplenic injection (n = 6–7 per treatment).

(M and N) PBS- or suramin-treated WT mice liver weight (M) and CRC foci coverage (N) on day 21 after intrasplenic MC38 injection (n = 6–8 mice per treatment).

(O and P) WT or *P2xr7*$^{-/-}$ mice liver weight (O) and metastatic foci coverage (P) on day 21 after intrasplenic injection of MC38 cells (n = 5–6 mice per genotype). Graphs represent the mean ± SEM. Statistical analysis was performed by Student's t test; *p < 0.05, ***p < 0.0001. All experiments were repeated two to three times, except for the experiment in (J) that was done once. See also Figure S2.

of Nlrp3 inflammasome-mediated anti-tumor immunity after chemotherapy (Ghiringhelli et al., 2009). To explore the specific contribution of ATP signaling to the control of CRC hepatic growth, we examined the response of *P2rx7*$^{-/-}$ mice, which are deficient in the purinergic receptor P2x7r, a ligand-gated ion channel that activates Nlrp3 after ATP binding (Ferrari et al., 2006; Martinon et al., 2009). Surprisingly, *P2rx7* was dispensable for tumor control (Figures 2O and 2P), suggesting either that

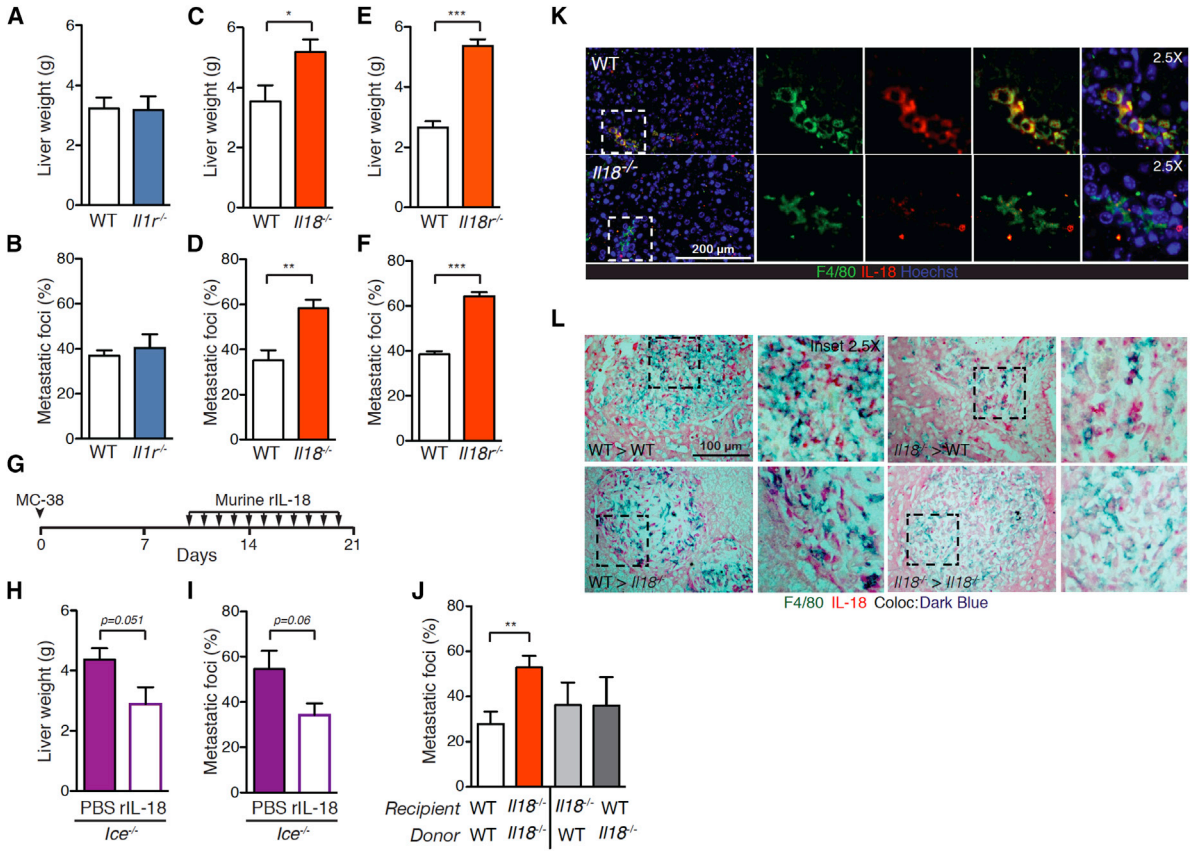

Figure 3. The Inflammasome Tumor-Suppressive Function Is Mediated by IL-18 Production by Radio-Sensitive and Radio-Resistant Cells

(A–F) *Il1r1*$^{-/-}$ mice (A, B), *Il18*$^{-/-}$ mice (C, D), or *Il18r1*$^{-/-}$ mice (E, F) liver weight (A, C, E) and CRC foci coverage (B, D, E) compared to WT mice on day 21 after intrasplenic injection of MC38 cells (n $\geq$ 6 mice per genotype per experiment).

(G) Schematic representation of the murine recombinant IL-18 (rIL-18) dosing schedule. *Ice*$^{-/-}$ mice were injected with MC38 cells on day 0. From day 10 until day 20, i.p. injections of 0.25 μg murine rIL-18 in 50 μl PBS were performed.

(H and I) PBS- or rIL-18-treated *Ice*$^{-/-}$ mice liver weight (H) and CRC foci coverage (I) on day 21 after intrasplenic MC38 injection (n = 5 mice per treatment).

(J) Bone marrow chimeric mice CRC foci coverage on day 21 after intrasplenic MC38 injection (n = 4–8 per group).

(K) Epifluorescence images of MC38 foci from WT or *Il18*$^{-/-}$ mice on day 21 post-injection using antibodies to mark macrophages (F4/80, green), IL-18 (red), and Hoechst (blue) staining for the nuclei. Insets correspond to boxed regions; scale bar represents 200 μm.

(L) Photomicrographs of immunohistochemical staining of mouse liver tissue sections from chimeric mice of the indicated genotype showing IL-18 (Permanent Red) and F4/80 (Emerald Green) expression. Cells expressing both proteins are in dark blue. Insets (zoom 2.5×) correspond to boxed regions; scale bar represents 100 μm.

Graphs represent the mean ± SEM. Statistical analysis was performed via Student's t test; *p < 0.05, **p < 0.001, ***p < 0.0001. All experiments were repeated two to three times, except for the experiment in (J) that was done once.

broad-spectrum inhibition of ATP receptors was required for tumor suppression or that suramin exerted its effects through an alternate pathway. Collectively, these results indicate that the Nlrp3 inflammasome is primed by tumor cells and is required to suppress CRC metastatic growth in the liver.

IL-18 Is Required for an Effective Inflammasome-Mediated Suppression of CRC Growth in the Liver

To identify the target(s) of caspase-1 responsible for controlling CRC metastatic growth in the liver, we first examined the contribution of its two canonical substrates, IL-1β and IL-18, by exploring the phenotype of *Il1r1*$^{-/-}$, *Il18*$^{-/-}$, and *Il18r*$^{-/-}$ mice. In contrast to *Il1r1*$^{-/-}$ mice (insensitive to both IL-1α and IL-1β), which are not different from WT animals in their ability to restrict tumor growth (Figures 3A and 3B), ablation of IL-18 signaling was deleterious; it resulted in larger metastatic tumor coverage in the livers of *Il18*$^{-/-}$ and *Il18r*$^{-/-}$ mice (Figures 3C–3F). To further confirm that the susceptibility of *Ice*$^{-/-}$ mice was due to lack of IL-18 production, we performed a rescue experiment, in which 0.25 μg of murine recombinant IL-18 (rIL-18) was administered daily from days 10 to 20 (Figure 3G). rIL-18 reduced the CRC burden in the liver of *Ice*$^{-/-}$ mice from 55% in vehicle-injected controls to 34% foci coverage (Figures 3H and 3I), which is similar to the tumor burden observed in WT mice (Figures 3B, 3D, and 3F). Next, to determine the cellular compartment required for the secretion of IL-18 in the liver, we generated bone marrow chimeras and investigated their response to MC38 intrasplenic cell injection. As expected, control *Il18*$^{-/-}$ mice receiving *Il18*$^{-/-}$ bone marrow (*Il18*$^{-/-}$ > *Il18*$^{-/-}$) had larger metastatic foci coverage in the liver than control WT

mice transplanted with WT bone marrow (WT > WT). On the other hand, *Il18*$^{-/-}$ mice receiving WT bone marrow (WT > *Il18*$^{-/-}$) and WT recipients of IL-18-deficient bone marrow (*Il18*$^{-/-}$ > WT) had similar phenotypes (Figure 3J). This suggested that IL-18 expression in both the radiosensitive and radioresistant compartments is required for anti-metastatic control. Immunofluorescence staining of tissue sections from tumor-bearing mice revealed that F4/80^{+} myeloid cells are the prevalent producers of IL-18 in the liver (Figure 3K), consistent with previous reports localizing Nlrp3 inflammasome activation to Kupffer cells (Huang et al., 2013; Kim et al., 2015). Bone marrow chimeras and orthotopic liver transplantation studies have previously distinguished two subsets of Kupffer cells, the first radioresistant and long-lived originating from intra-hepatic precursors and the second radiosensitive and rapidly replaced from hematopoeitic precursors (Klein et al., 2007). Examination of liver tissue sections from *Il18*$^{-/-}$ > WT chimeric mice revealed the presence of an IL-18^{+}F4/80^{+} sub-population of cells, consistent with incomplete depletion of IL-18-expressing macrophages by irradiation (Figure 3L). Thus, Kupffer cell heterogeneity might underlie the intermediate tumor control phenotype observed in our bone marrow chimera experiment. However, we cannot exclude that other radioresistant cells might also be involved.

Control of Hepatic Metastasis Occurs Independently of the Adaptive Immune System

IL-18 was initially discovered because of its ability to enhance IFN-γ production by CD8^{+} T cells and NK cells after stimulation with IL-12 (Novick et al., 2013). Because the requirement for the adaptive immune system has not been previously explored in this system, we tested the response of *Rag1*$^{-/-}$ mice to intrasplenic injection of MC38 cells. Interestingly, the metastatic burden observed in *Rag1*$^{-/-}$ mice was similar to that of WT animals (Figures S3A and S3B), suggesting that T, B, and NKT cells are not required for the suppression of MC38 liver metastatic growth. To confirm that IL-18 exerted its effects through the innate immune system, we next generated *Rag1*$^{-/-}$*Il18*$^{-/-}$ mice and assessed their tumor control response. Unlike *Rag1*$^{-/-}$ mice, *Rag1*$^{-/-}$*Il18*$^{-/-}$ mice exhibited increased liver weight and a larger MC38 foci area (Figures 4A and 4B). To explore the impact of impaired inflammasome signaling on innate immune cell subsets in the liver, we examined by flow cytometry the frequencies and absolute numbers of tumor-infiltrating leukocytes (TILs) in the liver of WT or *Ice*$^{-/-}$ mice. No significant differences were found for NK cells, inflammatory monocytes, neutrophils, resident macrophages, or dendritic cells between WT and *Ice*$^{-/-}$ mice (Figures 4C, 4D, S4A, and S4B). Because of the critical tumoricidal role of NK cells, we further examined their maturation in the liver. Murine NK cells acquire effector functions after a 4-stage maturation process from CD11b^{lo}CD27^{lo} → CD11b^{lo}CD27^{hi} → CD11b^{hi}CD27^{hi} → CD11b^{hi}CD27^{lo}, with the latter being fully mature cytotoxic NK cells (Chiossone et al., 2009). FACS staining of hepatic NK cells on day 14 p.i. showed a decrease in the frequencies and numbers of fully activated NK cells (CD11b^{hi}CD27^{lo}) in *Ice*$^{-/-}$ mice compared to WT animals (Figures 4E–4G). Staining for KLRG1 and CD69, a marker for NK cell cytotoxic activity, also revealed decreased frequencies of CD69^{hi}KLRG1^{lo} hepatic NK cells in *Ice*$^{-/-}$ mice compared to WT animals (Figures 4H–4J). This NK cell phenotype was restricted to hepatic NK cells in tumor-bearing mice at day 14 p.i., as indicated by the fact that the maturation or activation of peripheral blood NK cells at this time point was similar in WT and *Ice*$^{-/-}$ mice (Figures S3C and S3D). Furthermore, no differences in NK cell maturation were observed under steady-state conditions (day 0) in the liver, blood, or spleen (Figures S3E and S3F). Surprisingly, the ability of NK cells to produce IFN-γ after isolation from the liver and either restimulation with PMA/ionomycin (Figures 4K and 4L) or plate-bound NK1.1 (Figures 4M, 4N, and S3G) was not affected in *Ice*$^{-/-}$ mice. Consistently, although increased hepatic tumor load was observed in *Ifng*$^{-/-}$ mice, administration of recombinant IL-18 to these mice exerted tumor suppression (Figures S3H and S3I), suggesting that IL-18 operated independently of IFN-γ-mediated tumor control mechanisms. Similarly, the lytic activity of liver NK cells from either genotype on RMA cells was similar (Figure S3J), consistent with unimpaired function of granzymes and perforin, which are the primary executors in this killing assay (Wallin et al., 2003). Collectively, our results suggest that IL-18 mediates its tumor-suppressive function independently of the adaptive immune system or IFN-γ signaling. Our data also show that impairment of inflammasome signaling impacts the maturation of hepatic NK cells in tumor-bearing mice.

IL-18 Acts on NK Cells to Control CRC Metastasis to the Liver

NK cells have been shown to positively correlate with patient survival in numerous cancers (Imai et al., 2000). To determine the contribution of NK cells to the control of MC38 hepatic metastasis, we examined the response of *Jak3*^{W81R} mice, which lack NK cells while also lacking adaptive immune effectors (Bongfen et al., 2012). Unlike *Rag1*$^{-/-}$ mice, *Jak3*^{W81R} mice had an increased metastatic burden as early as day 19 p.i. (Figures 5A and 5B), indirectly implicating NK cells in suppressing tumorigenesis. To confirm a role for NK cells in tumor immunosurveillance in this model, we administered the NK-cell-depleting anti-asialo GM1 (αGM1) antibody to WT mice and determined their response to MC38 liver growth. Consistent with the results obtained with *Jak3*^{W81R} mice, depletion of NK cells in WT animals increased their metastatic burden compared to PBS-treated controls (Figures 5C and 5D). Moreover, the adoptive transfer of WT splenocytes into *Jak3*^{W81R} mice reduced their liver metastatic burden significantly compared to that of *Il18r*$^{-/-}$ splenocytes (Figure 5E), indicating that IL-18 signaling on NK cells is needed to control MC38 liver growth. We next addressed whether IL-18 exerted additional functions on tumor control beyond a NK-cell-mediated effect. To do so, we depleted NK cells prior to injecting MC38 cells into *Ice*$^{-/-}$ mice using αGM1 and subsequently administered rIL-18 from day 10 to day 19 (Figure 5F). As expected, ending the experiment on day 19 p.i. resulted in a smaller tumor burden in *Ice*$^{-/-}$ mice (Figures 5G and 5H) compared to their observed load on day 21 p.i. (Figures 1F, 1G, and S1A), providing a window to observe further increase in tumorigenesis due to NK cell depletion. Interestingly, rIL-18 administration did not alter the metastatic phenotype of NK-cell-depleted *Ice*$^{-/-}$ mice (Figures 5G and 5H), in contrast to what was observed in NK-cell-replete *Ice*$^{-/-}$ mice (Figures 3G–3I). To further demonstrate that IL-18 signaling is required directly on NK cells, we generated *Il18r*$^{-/-}$*Il15r*$^{-/-}$ > WT mixed

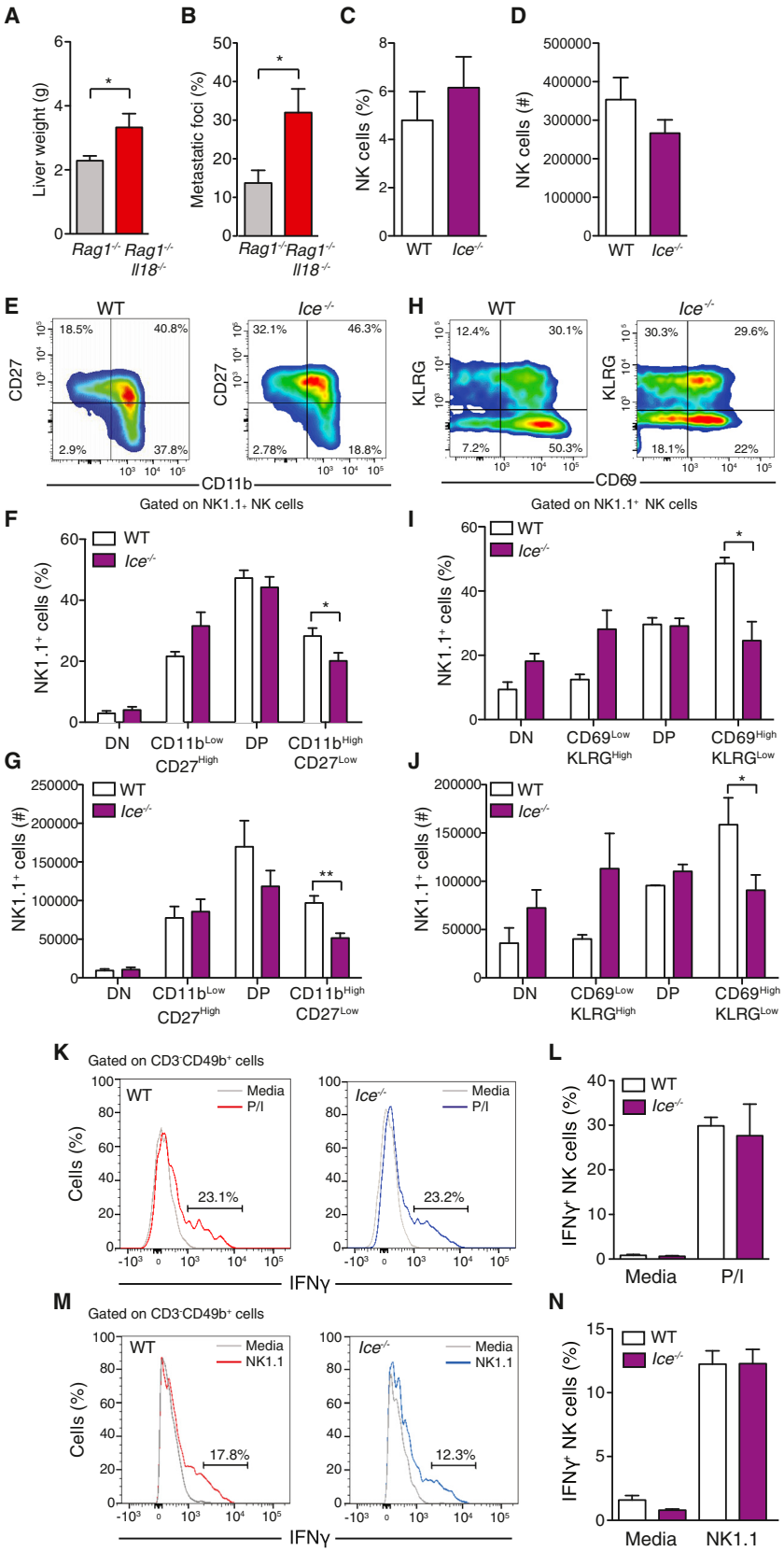

Figure 4. Restriction of Colorectal Cancer Growth in the Liver Occurs Independently of the Adaptive Immune System and IFN-γ Production

(A and B) *Rag1*$^{-/-}$ and *Rag1*$^{-/-}$*Il18*$^{-/-}$ mice liver weight (A) and CRC foci coverage (B) on day 21 after intrasplenic injection of MC38 cells (n = 6–8 mice per genotype).

(C and D) Percentages (C) and absolute numbers (D) of NK cells (NK1.1^{+} cells) in the liver of WT or *Ice*$^{-/-}$ mice 14 days after intrasplenic injection of MC38 cells.

(E) Representative FACS plots of CD11b and CD27 NK1.1^{+} cells in liver leukocytes from WT or *Ice*$^{-/-}$ mice collected on day 14 after MC38 intrasplenic injection.

(F and G) Percentages (F) and absolute numbers (G) of NK cells according to their maturation phenotype. Double negative (DN), CD11b^{-}CD27^{-}; double positive (DP), CD11b^{+}CD27^{+} (n = 5 per genotype).

(H) Representative FACS plots of CD69 and KLRG1 NK1.1^{+} cells in liver leukocytes from WT or *Ice*$^{-/-}$ mice collected on day 14 after MC38 intrasplenic injection.

(I and J) Percentages (I) and absolute numbers (J) of NK cells according to their expression of CD69 and KLRG1 (n = 3 per genotype).

(K–N) Representative histograms (K, M) and quantification graph (L, N) of IFN-γ production by NK cells after overnight stimulation of liver leukocytes purified on day 14 post-MC38 intrasplenic injection from WT or *Ice*$^{-/-}$ mice with PMA/ionomycin (P/I) (K, L) or plate-bound NK1.1 (M, N) (n = 5 mice per genotype). Graphs represent the mean ± SEM. Statistical analysis was performed by Student's t test; *p < 0.05. All experiments were repeated two to three times. See also Figure S3.

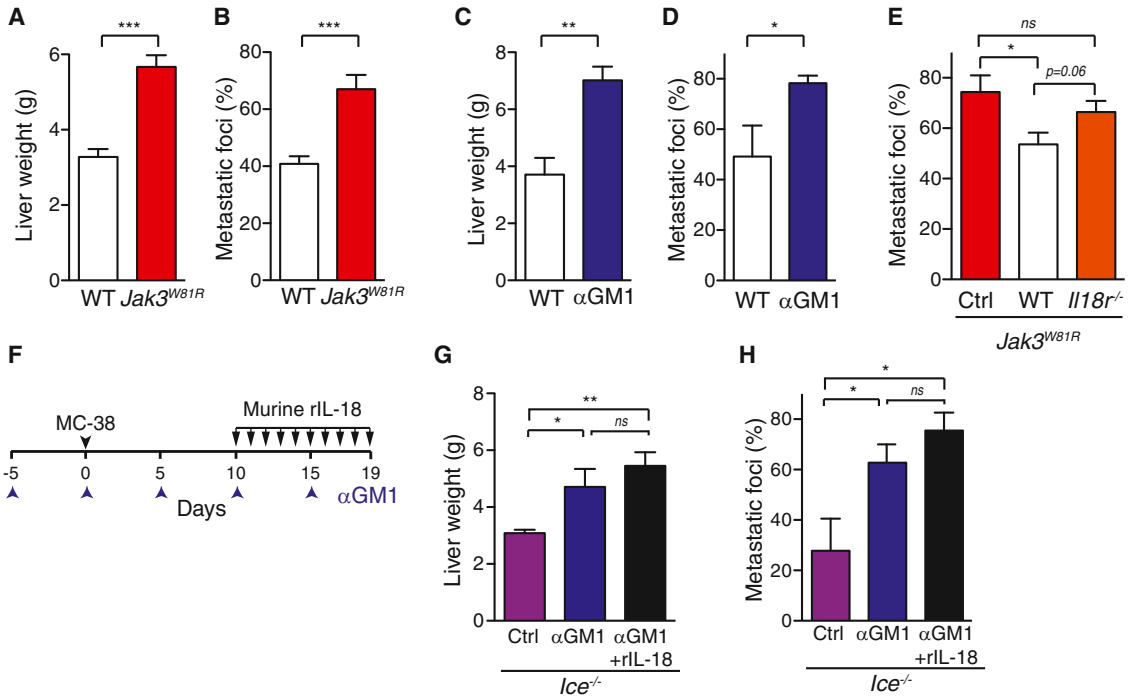

Figure 5. IL-18 Mediates Natural Killer Cell Tumoricidal Activity in the Liver

(A and B) WT or *Jak3*^{W81R} mice liver weight (A) and CRC foci coverage (B) on day 19 post-MC38 intrasplenic injection (n = 4–7 mice per genotype).

(C and D) PBS- or anti-asialo GM1-treated WT mice liver weight (C) and CRC foci coverage (D) on day 19 post-MC38 intrasplenic injection (n = 6–7 mice per treatment).

(E) CRC foci coverage on day 19 in *Jak3*^{W81R} mice that received PBS injection (Ctl) or splenocyte adoptive transfers 5 days post-MC38 intrasplenic injection. The data are pooled from two experiments (n = 7–10 mice per genotype).

(F) Schematic representation of rIL-18 dosing schedule in Ctl or NK cell-depleted *Ice*$^{-/-}$ mice. Starting on day −5, *Ice*$^{-/-}$ mice were administered with anti-asialo GM1 antibodies i.p. every 5 days. On day 0, MC38 cells were intrasplenically injected, and on day 10, mice received i.p. daily injections of either PBS or rIL-18.

(G and H) Liver weight (G) and CRC foci coverage (H) of *Ice*$^{-/-}$ mice replete or deplete of NK cells and receiving or not rIL-18 was determined on day 19 after MC38 intrasplenic injection (n = 3–5 mice per group).

Graphs represent the mean ± SEM. Statistical analysis was performed by Student's t test; *p < 0.05, **p < 0.001, ***p < 0.0001, ns, not significant. All experiments were repeated two to three times. See also Figure S4.

bone marrow chimeras to deplete IL-18r expression specifically on NK cells (Figures 6A–6C). As expected, loss of *Il18r* on NK cells recapitulated the impairment in immunosurveillance observed in inflammasome signaling-deficient mice or mice lacking NK cells (*Il15ra*$^{-/-}$ > WT, Figure 6C). Overall, this suggests that IL-18 signaling on NK cells contributes to the control of MC38 metastatic growth in the liver.

NK Cell Tumoricidal Function Is Mediated by IL-18 Signaling of FasL Cytotoxicity

Because we observed that the capacity of hepatic NK cells to produce IFN-γ was unaffected in *Ice*$^{-/-}$ mice (Figures 4K–4N) and that recombinant IL-18 treatment of *Ifng*$^{-/-}$ mice was effective at reducing tumor burden (Figure S3I), we hypothesized that IL-18 regulated NK cell lytic activity independently of IFN-γ. Interestingly, it was previously shown that suramin, which we used as a putative P2 blocker and that significantly increased MC38 metastatic liver growth (Figures 2M and 2N), inhibited Fas-induced apoptosis (Eichhorst et al., 2004). Furthermore, Smyth et al. (2004) have previously reported an IFN-γ-independent function of IL-18 in mediating NK cell suppression of metastasis that required tumor cell sensitivity to Fas ligand (FasL). Although ex vivo treatment of splenic NK cells with IL-18 for 45 min robustly induced *Ifng* expression in WT but not *Il18r*$^{-/-}$ NK cells, as predicted, it did not impact *Fasl* expression at this time point, as determined by qPCR analysis (Figures 6D and 6E). In contrast, IL-18 stimulated a rapid and robust upregulation of FasL protein on the surface of NK cells, which occurred within 45 min of stimulation, as measured by FACS analysis of the mean fluorescence intensity (MFI) of FasL (Figures 6F and 6G). To interrogate whether inflammasome-mediated metastasis control was mediated by FasL-induced cytotoxicity, we first determined the sensitivity of MC38 cells to FasL killing in vitro. As shown in Figure S5A, treatment of MC38 cells with FasL (10 ng/ml) induced approximately 50% cell death, as quantified by propidium iodide (PI) staining and FACS. In contrast, the murine rectal carcinoma CMT93 cells were markedly resistant to FasL-induced cell death (Figure S5A). Consistent with a role for FasL-mediated NK cytotoxicity in the control of MC38 metastatic growth, *Fasl*$^{gld/gld}$*Il15r*$^{-/-}$ > WT mixed bone marrow chimeras failed to control MC38 metastatic liver growth (Figure 6C). Collectively, our results demonstrate that IL-18 signaling regulates FasL surface expression on NK cells, which contributes to their tumoricidal function and suppression of CRC liver growth.

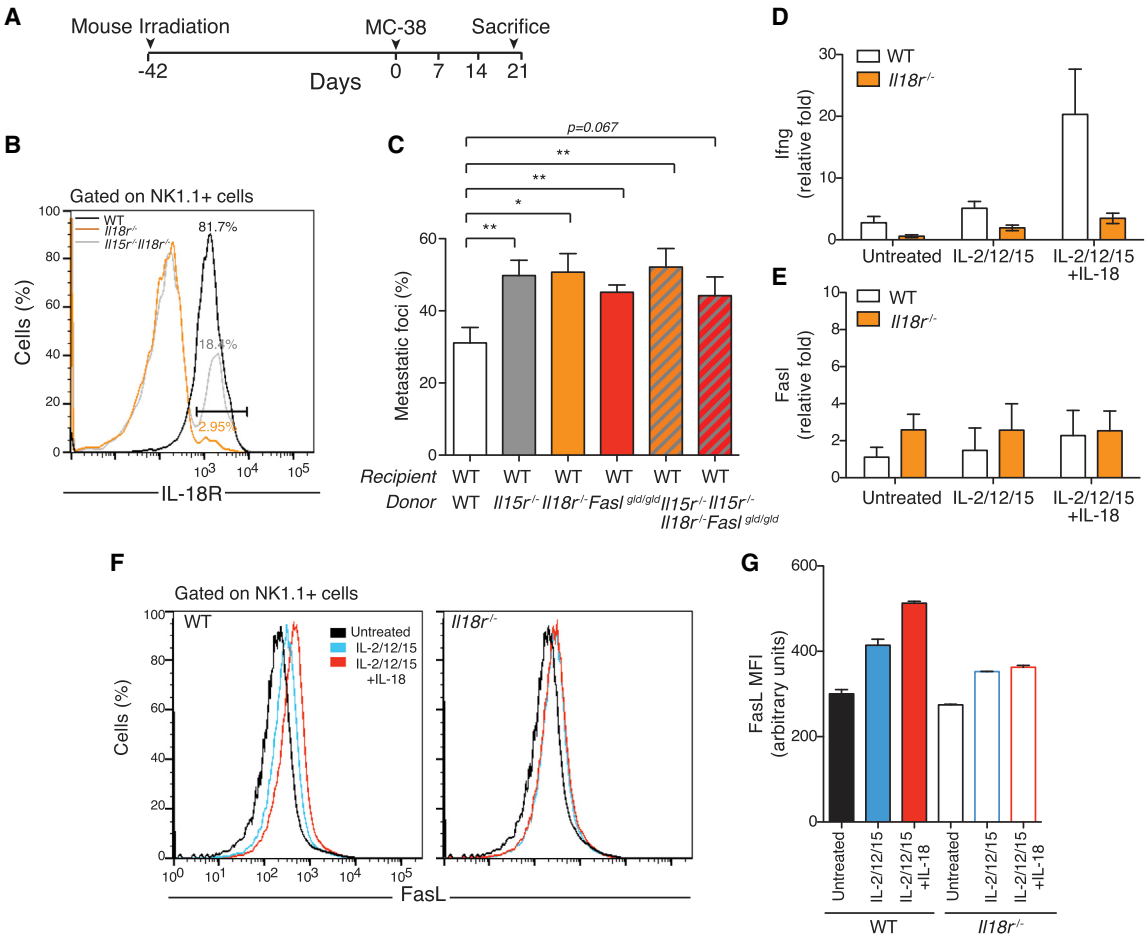

Figure 6. Expression of IL-18r by NK Cells and FasL Are Required for CRC Growth Restriction in the Liver

(A) Schematic representation of experimental layout. Mice were irradiated and reconstituted with bone marrow from WT (n = 9), *Il15ra*$^{-/-}$ (n = 9), *Il18r1*$^{-/-}$ (n = 8), *Fasl*$^{gld/gld}$ (n = 10), or a 1:1 cell ratio of *Il15ra*$^{-/-}$:*Il18r1*$^{-/-}$ (n = 9) or *Il15ra*$^{-/-}$:*Fasl*$^{gld/gld}$ (n = 9) mice 6 weeks prior to intrasplenic injection of MC38 cells.

(B) Representative FACS plots of IL-18r-expressing NK1.1^{+} cells in the spleen from WT bone marrow chimeric mice collected on the day of MC38 intrasplenic injection.

(C) CRC foci coverage in chimeric mice on day 19 after MC38 intrasplenic injection. Graphs represent the mean ± SEM. Statistical analysis was performed by Student's t test; *p < 0.05, **p < 0.001.

(D and E) mRNA derived from untreated NK cells or NK cells treated with IL-2, IL-12, and IL-15 or with IL-2, IL-12, IL-15, and IL-18 from WT (n = 5) or *Il18r*$^{-/-}$ (n = 3) mice 45 min after treatment was analyzed for the expression of *Ifng* (D) and *Fasl* (E).

(F and G) Representative histogram (F) and mean fluorescence intensity (G) of FasL expression on WT (n = 5) or *Il18r*$^{-/-}$ (n = 3) NK cells, before or 45 min after treatment with IL-2, IL-12, and IL-15 or with IL-2, IL-12, IL-15, and IL-18.

See also Figure S5.

To confirm that the susceptibility phenotype of *Ice*$^{-/-}$ mice was determined by the sensitivity of tumor cells to FasL, we examined the response of WT and *Ice*$^{-/-}$ mice to intrasplenic injection of FasL-insensitive CMT93 cells. Consistent with our hypothesis, *Ice*$^{-/-}$ mice had a similar hepatic metastatic burden compared to WT mice when FasL-resistant tumor cells were used in this liver metastasis model (Figures S5B and S5D). We further tested the sensitivity of Lewis lung carcinoma (LLC) cells to FasL and found that, like MC38 cells, they were highly sensitive to Fas-induced killing (Figure S5A), consistent with a previous report (Smyth et al., 2004). This allowed us to interrogate whether inflammasome-mediated anti-metastatic control was tissue specific. After intravenous injection of LLC cells that home to the lung, *Ice*$^{-/-}$ mice had a significantly higher metastatic burden than WT mice on day 28 p.i. (Figures S5E and S5F). Collectively, these results suggested that the sensitivity of tumor cells to FasL is a determinant of whether caspase-1 activation and subsequent IL-18 release contributes to control of metastatic growth in secondary organs.

DISCUSSION

Colorectal cancer-associated deaths occur due to its dissemination to secondary organs, primarily the liver (Manfredi et al., 2006; Tsikitis et al., 2014). Through investigation of the function of the inflammasome pathway in an experimental animal model of CRC metastatic liver growth, we have genetically delineated a circuitry in the innate immune system linking sensing of danger

signals by the Nlrp3 inflammasome to activation of hepatic NK cell cytolytic activity required for metastatic control. Inflammasome-mediated tumor suppression required IL-18 signaling on NK cells but was independent of IFN-γ production. Instead, IL-18 promoted NK cell maturation and primed their tumoricidal function, which required FasL-sensitive tumor cells.

The liver is constantly exposed to intestinal microbial products through the portal vein circulation, but its unique tolerogenic environment prevents unwanted immune responses. Engagement of the inflammatory caspase pathway after CRC liver colonization indicated inflammasome activation by a danger signal emanating in response to metastatic lesion formation. In this model, we have ruled out the contribution of cytosolic DNA sensing by Aim2 or recognition of flagellated bacteria by Nlrc4, because ablation of either's gene was dispensable for metastatic control.

The Nlrp3 inflammasome is activated by a wide spectrum of agonists including both microbial and sterile triggers (Latz et al., 2013). The microbiota has surfaced in recent years as an important determinant of health and disease. Notably, it was recently demonstrated that antibiotic-treated or germ-free mice respond poorly to cancer immunotherapy and chemotherapy. The commensal microbiota was required for promoting cytotoxicity after chemotherapy by modulating the tumor microenvironment (Iida et al., 2013; Viaud et al., 2013). Although significant depletion of bacterial content with the use of antibiotics was achieved in our experiments, it did not modulate the anti-metastatic response, suggesting that Nlrp3 activation was not impaired by deregulation of the microbial ecology. However, we cannot exclude that Nlrp3 activation might be mediated by a microbial ligand derived from the remaining intestinal microbiota. The production of ROS has been linked to cancer promotion and in some cases to the activation of the Nlrp3 inflammasome (Fang et al., 2009). Similarly, uric acid is a principal endogenous DAMP released from injured cells (Shi et al., 2003) and along with ROS was considered herein as a potential DAMP upstream of Nlrp3 activation in the tumor microenvironment. However, treatment with NAC or allopurinol, a uric acid analog that reduces uric acid production, did not affect the formation of metastatic foci. Although a number of Nlrp3 agonists, including microbial triggers, were previously reported to require extracellular ATP and P2X7 receptor signaling for inflammasome activation (Latz et al., 2013), ablation of *P2xr7* did not inhibit the inflammasome in our model, as shown by the fact that *P2xr7*$^{-/-}$ mice did not phenocopy *Nlrp3*$^{-/-}$ or *Ice*$^{-/-}$ animals and were equivalent to WT animals in their metastatic burden. Surprisingly, suramin, which has been commonly used as a putative P2 receptor blocker in studies interrogating Nlrp3 inflammasome activation by ATP (Coddou et al., 2011), had a striking effect on tumor evasion. Interestingly, suramin was previously investigated for its anti-tumorigenic properties in adrenocortical and prostate cancer and was reported to inhibit death receptor-induced apoptosis by modulating activation of caspase-8 within the death-inducing signaling complex (DISC) (Eichhorst et al., 2004). Although we could not identify the agonist that activated the Nlrp3 inflammasome, we demonstrated that colorectal cancer cells primed the inflammasome. This is in accordance with a previous report demonstrating that tumor cells promoted inflammation and tumorigenesis through the secretion of factors that engaged the NF-κB pathway (Kim et al., 2009).

The anti-tumorigenic activity of IL-18 has been classically linked to its IFN-γ-inducing capacity both in cytotoxic T cells and NK cells (Novick et al., 2013). Control of liver metastatic growth occurred independently of T, B, and NKT cells but required NK cells. Interestingly, although NK cells from inflammasome-deficient mice were impaired in controlling MC38 liver cell growth, their IFN-γ production was intact and their ability to kill RMA cells was similar to that of WT mice. Of note, RMA cells are insensitive to Fas-induced cytotoxicity but killed by NK cells through perforin- and granzyme-mediated cytotoxicity (Wallin et al., 2003). Interestingly, our results showed that the anti-metastatic function of inflammasome signaling required FasL-sensitive tumor cells. Notably, *Ice*$^{-/-}$ mice were equivalent to WT animals in their ability to control metastatic growth of FasL-resistant tumor cells, suggesting that IL-18 production has otherwise a minimal impact on immunosurveillance in this model. Mechanistically, IL-18 controls a rapid FasL expression on the surface of NK cells, potentially through relocation of intracellular FasL stores, as previously described in cytotoxic T lymphocytes (He et al., 2010). Notably, the site of IL-18 production, and likely its local concentration, greatly affects metastasis outcome. For instance, in contrast to host-derived IL-18, which we show in this model to be anti-metastatic, IL-18 production by cancer cells was shown to promote melanoma liver metastasis in an animal model (Valcárcel et al., 2014), and an IL-18-dependent gene expression signature was shown to correlate with invasive human melanoma (Crende et al., 2013). Additionally, in a model of lung metastasis, IL-18 production by cancer cells was reported to induce the development of an immature population of NK cells, which promoted metastasis (Terme et al., 2011, 2012). This highlights the heterogeneity of cancer cell responses to IL-18 and the ability of this immunoregulatory cytokine to positively or negatively affect the outcome of metastasis.

FasL plays a crucial role in cellular homeostasis and immune surveillance by inducing cell death through its receptor Fas. As such, the therapeutic potential of FasL has been explored to target tumor cells. However, this approach has had limitations, because of hepatotoxicity. Interestingly, tumor cells usurp the FasL-Fas pathway to their advantage. For instance, some colon cancer cells upregulate FasL on their surface to facilitate seeding in the liver by promoting epithelial-mesenchymal transition (Zheng et al., 2013) and inducing hepatocyte cell death (Li et al., 2009). In addition, to evade immunosurveillance mediated by FasL killing, these tumor cells also express decoy receptors and c-FLIP. This not only ensures cancer cell survival and resistance to Fas-induced cell death, but also promotes Fas-driven cell proliferation (Li et al., 2009).

Harnessing the immune system to fight cancer and metastatic growth is the next breakthrough in cancer therapy. However, this can be achieved only by in-depth characterization of cancer cells in relation to their microenvironment. Here, we have provided a model view of how the inflammasome, IL-18, and FasL can be utilized against certain types of metastatic cancer to enhance immune surveillance. To gain a more complete picture of the significance of this mechanism in metastasis control, it will be important to determine the impact of inflammasome component

expression and activation in conjunction with the status of death receptor pathway effectors on cancer progression and patient outcome.

EXPERIMENTAL PROCEDURES

Mice

Animals used throughout the study were sex-matched 6- to 12-week-old mice on a C57BL6/J background and bred as separate colonies. C57BL6/J, *Rag1*$^{-/-}$, *Il1r1*$^{-/-}$, *Il18*$^{-/-}$, *Il18r1*$^{-/-}$, *P2xr7*$^{-/-}$, and *Fasl*$^{gld/gld}$ mice were obtained from The Jackson Laboratory. *Ice*$^{-/-}$ mice were obtained from R. Flavell (Yale University) (Kuida et al., 1995). *Nlrp3*$^{-/-}$, *Nlrc4*$^{-/-}$, and *Aim2*$^{-/-}$ mice were from Genentech. *Jak3*^{W81R} mice were generated through an ENU screen, as previously reported (Bongfen et al., 2012). All of the above mouse strains were bred in house and experiments were performed according to the guidelines of the Animal Ethics committee of McGill University (Canada). *Il15ra*$^{-/-}$ mice were maintained at the University of Connecticut Health Center (Lodolce et al., 1998).

Animal Models

To induce the development of liver metastasis, mice were injected intrasplenically with 2×10^5 MC38 or 1.5×10^6 CMT93 cells in 50 μl of phosphate-buffered saline (PBS), followed by splenectomy 3 min after injections. PBS-injected mice served as controls. Mice were sacrificed 14 or 21 days after the initial injection. For the induction of lung metastasis, 2×10^5 LLC cells (ATCC) in 100 μl PBS were injected intravenously (i.v.) and mice were sacrificed 21 days later. To quantify the metastatic burden, H&E slides were scanned with ScanScope XT (Aperio Technologies). To calculate the metastatic burden with the ImageScope software, the area occupied by metastatic foci was divided by the total surface area. For adoptive transfer, 20×10^6 splenocytes from donor mice were injected i.v. on day 5. Where indicated, 0.25 μg of mouse recombinant IL-18 (MBL, B002-5) was injected intraperitoneally (i.p.) daily between days 10 and 20 or 1 mg suramin (Sigma, S2671) was injected i.p. three times per week, starting on the day of the intrasplenic injection. 1% (weight/volume) NAC (Sigma, A7250) was added to the drinking water of the animals. 10 g/kg of allopurinol (Sigma, A8003) was given i.p. daily starting on day 10.

Generation of Bone Marrow Chimeras

3 days prior to irradiation, 1 mg/ml sulfamethoxazole (Sigma, S7507) and 0.2 mg/ml trimethoprim (Sigma, T7883) were given in the drinking water. Mice were kept on this regimen for an additional 3 weeks. Recipient mice were lethally irradiated in the afternoon with 1,000 rads using the X-Ray RS-2000 Biological irradiator. The next morning, red-blood-cell-depleted bone marrow from sex-matched donor mice was injected i.v. (ratio of one donor for three recipients). For the mixed bone marrow experiment, a 1:1 *Il15r*$^{-/-}$:*Il18r*$^{-/-}$ or *Fasl*$^{gld/gld}$ ratio was used. The extent of engraftment was verified after 6 weeks by FACS staining of blood lymphocytes.

Depletion of NK Cells

50 μl anti-asialo GM1 (Wako Chemicals, Cat #986-10001)/mouse was injected i.p. every 5 days starting 5 days prior to the intrasplenic injection. Confirmation of NK cell depletion in the spleen was performed after splenectomy on day 0 and in the liver at endpoint.

NK Isolation

For the lytic assay, target RMA cells were labeled with the cell proliferation dye eFluor 670 (eBioscience cat# 65-0840). Liver NK cells were isolated with NK cell isolation II (Miltenyi biotech cat#130-096-892) with autoMACS and incubated with target cells at a ratio of 20:1 for 4 hr at 37°C. Cells were then stained with 7-AAD (eBioscience, 00-6993-50) to quantify cell death. For the ex vivo restimulation, splenic NK cells were isolated as above and stimulated with 20 ng/ml IL-2 (Preprotech, 212-12), 10 ng/ml IL-12 (Preprotech, 210-12), 50 ng/ml of IL-15 (210-15), and 50 ng/ml of IL-18 (MBL, B002-5) in complete media for 45 min prior to RNA isolation or FACS analysis.

Quantitative Real-Time PCR

Total RNA (2 μg) was reverse transcribed with M-MLV reverse transcriptase (InVitrogen, Cat# 28025-013) and random hexamers in a volume of 20 μl according to the manufacturer's protocol. The primers used for quantitative real-time PCR are available upon request. All reactions were normalized to the housekeeping gene *L32* to quantify the relative gene expression and were then analyzed by the $2^{-\Delta\Delta CT}$ method.

Statistical Analysis

Data are represented as mean ± standard error of the mean (SEM). Two-tailed Student's t test was used for evaluating statistical significance between groups. *$p < 0.05$; **$p < 0.001$; ***$p < 0.0001$; n.s., not significant. All experiments were repeated twice or more unless otherwise specified in the figure legends.

SUPPLEMENTAL INFORMATION

Supplemental Information includes five figures and Supplemental Experimental Procedures and can be found with this article online at http://dx.doi.org/10.1016/j.immuni.2015.08.013.

ACKNOWLEDGMENTS

We thank Dr. V. Dixit and Genentech for providing *Nlrc4*$^{-/-}$*Nlrp3*$^{-/-}$ and *Aim2*$^{-/-}$ mice; Dr. Shoshana Yakar for MC38 cells; and J. Rinz and G. Perrault for animal husbandry. This work was supported by grants from the Canadian Institutes for Health Research (CIHR-MOP 82801 to M.S. and 86582 to N.B.) and the Burroughs Wellcome Fund to M.S., who is also a Fonds de Recherche du Québec en Santé (FRQS) Senior Investigator and a McGill University William Dawson Scholar. J.D.-C. and M.D. are supported by doctoral studentships from the CIHR. A.A. is supported by a postdoctoral fellowship from the FRSQ. I.G.R.-G. is supported by postdoctoral fellowships from the FRSQ, CIHR, and by the Strauss Foundation. A.M. was supported by a CIHR/CAG/Abbott fellowship. S.L.C. was supported by a postdoctoral fellowship from the American Cancer Society (Grant PF-11-152-01-LIB).

Received: November 20, 2014
Revised: May 7, 2015
Accepted: July 20, 2015
Published: September 15, 2015

REFERENCES

Allen, I.C., TeKippe, E.M., Woodford, R.M., Uronis, J.M., Holl, E.K., Rogers, A.B., Herfarth, H.H., Jobin, C., and Ting, J.P. (2010). The NLRP3 inflammasome functions as a negative regulator of tumorigenesis during colitis-associated cancer. J. Exp. Med. *207*, 1045–1056.

Balkwill, F., and Coussens, L.M. (2004). Cancer: an inflammatory link. Nature *431*, 405–406.

Bongfen, S.E., Rodrigue-Gervais, I.G., Berghout, J., Torre, S., Cingolani, P., Wiltshire, S.A., Leiva-Torres, G.A., Letourneau, L., Sladek, R., Blanchette, M., et al. (2012). An N-ethyl-N-nitrosourea (ENU)-induced dominant negative mutation in the JAK3 kinase protects against cerebral malaria. PLoS ONE *7*, e31012.

Carrascal, M.T., Mendoza, L., Valcárcel, M., Salado, C., Egilegor, E., Tellería, N., Vidal-Vanaclocha, F., and Dinarello, C.A. (2003). Interleukin-18 binding protein reduces b16 melanoma hepatic metastasis by neutralizing adhesiveness and growth factors of sinusoidal endothelium. Cancer Res. *63*, 491–497.

Chiossone, L., Chaix, J., Fuseri, N., Roth, C., Vivier, E., and Walzer, T. (2009). Maturation of mouse NK cells is a 4-stage developmental program. Blood *113*, 5488–5496.

Coddou, C., Yan, Z., Obsil, T., Huidobro-Toro, J.P., and Stojilkovic, S.S. (2011). Activation and regulation of purinergic P2X receptor channels. Pharmacol. Rev. *63*, 641–683.

Crende, O., Sabatino, M., Valcárcel, M., Carrascal, T., Riestra, P., López-Guerrero, J.A., Nagore, E., Mandruzzato, S., Wang, E., Marincola, F.M., and Vidal-Vanaclocha, F. (2013). Metastatic lesions with and without interleukin-18-dependent genes in advanced-stage melanoma patients. Am. J. Pathol. *183*, 69–82.

Dupaul-Chicoine, J., Yeretssian, G., Doiron, K., Bergstrom, K.S., McIntire, C.R., LeBlanc, P.M., Meunier, C., Turbide, C., Gros, P., Beauchemin, N., et al. (2010). Control of intestinal homeostasis, colitis, and colitis-associated colorectal cancer by the inflammatory caspases. Immunity *32*, 367–378.

Eichhorst, S.T., Krueger, A., Müerköster, S., Fas, S.C., Golks, A., Gruetzner, U., Schubert, L., Opelz, C., Bilzer, M., Gerbes, A.L., and Krammer, P.H. (2004). Suramin inhibits death receptor-induced apoptosis in vitro and fulminant apoptotic liver damage in mice. Nat. Med. *10*, 602–609.

Eisenbarth, S.C., and Flavell, R.A. (2009). Innate instruction of adaptive immunity revisited: the inflammasome. EMBO Mol. Med. *1*, 92–98.

Elinav, E., Strowig, T., Kau, A.L., Henao-Mejia, J., Thaiss, C.A., Booth, C.J., Peaper, D.R., Bertin, J., Eisenbarth, S.C., Gordon, J.I., and Flavell, R.A. (2011). NLRP6 inflammasome regulates colonic microbial ecology and risk for colitis. Cell *145*, 745–757.

Fang, J., Seki, T., and Maeda, H. (2009). Therapeutic strategies by modulating oxygen stress in cancer and inflammation. Adv. Drug Deliv. Rev. *61*, 290–302.

Ferlay, J., Soerjomataram, I., Dikshit, R., Eser, S., Mathers, C., Rebelo, M., Parkin, D.M., Forman, D., and Bray, F. (2015). Cancer incidence and mortality worldwide: Sources, methods and major patterns in GLOBOCAN 2012. Int. J. Cancer *136*, E359–E386.

Ferrari, D., Pizzirani, C., Adinolfi, E., Lemoli, R.M., Curti, A., Idzko, M., Panther, E., and Di Virgilio, F. (2006). The P2X7 receptor: a key player in IL-1 processing and release. J. Immunol. *176*, 3877–3883.

Galon, J., Angell, H.K., Bedognetti, D., and Marincola, F.M. (2013). The continuum of cancer immunosurveillance: prognostic, predictive, and mechanistic signatures. Immunity *39*, 11–26.

Ghiringhelli, F., Apetoh, L., Tesniere, A., Aymeric, L., Ma, Y., Ortiz, C., Vermaelen, K., Panaretakis, T., Mignot, G., Ullrich, E., et al. (2009). Activation of the NLRP3 inflammasome in dendritic cells induces IL-1beta-dependent adaptive immunity against tumors. Nat. Med. *15*, 1170–1178.

He, J.S., Gong, D.E., and Ostergaard, H.L. (2010). Stored Fas ligand, a mediator of rapid CTL-mediated killing, has a lower threshold for response than degranulation or newly synthesized Fas ligand. J. Immunol. *184*, 555–563.

Huang, H., Chen, H.W., Evankovich, J., Yan, W., Rosborough, B.R., Nace, G.W., Ding, Q., Loughran, P., Beer-Stolz, D., Billiar, T.R., et al. (2013). Histones activate the NLRP3 inflammasome in Kupffer cells during sterile inflammatory liver injury. J. Immunol. *191*, 2665–2679.

Huber, S., Gagliani, N., Zenewicz, L.A., Huber, F.J., Bosurgi, L., Hu, B., Hedl, M., Zhang, W., O'Connor, W., Jr., Murphy, A.J., et al. (2012). IL-22BP is regulated by the inflammasome and modulates tumorigenesis in the intestine. Nature *491*, 259–263.

Iida, N., Dzutsev, A., Stewart, C.A., Smith, L., Bouladoux, N., Weingarten, R.A., Molina, D.A., Salcedo, R., Back, T., Cramer, S., et al. (2013). Commensal bacteria control cancer response to therapy by modulating the tumor microenvironment. Science *342*, 967–970.

Imai, K., Matsuyama, S., Miyake, S., Suga, K., and Nakachi, K. (2000). Natural cytotoxic activity of peripheral-blood lymphocytes and cancer incidence: an 11-year follow-up study of a general population. Lancet *356*, 1795–1799.

Jenne, C.N., and Kubes, P. (2013). Immune surveillance by the liver. Nat. Immunol. *14*, 996–1006.

Keller, M., Rüegg, A., Werner, S., and Beer, H.D. (2008). Active caspase-1 is a regulator of unconventional protein secretion. Cell *132*, 818–831.

Kim, S., Takahashi, H., Lin, W.W., Descargues, P., Grivennikov, S., Kim, Y., Luo, J.L., and Karin, M. (2009). Carcinoma-produced factors activate myeloid cells through TLR2 to stimulate metastasis. Nature *457*, 102–106.

Kim, H.Y., Kim, S.J., and Lee, S.M. (2015). Activation of NLRP3 and AIM2 inflammasomes in Kupffer cells in hepatic ischemia/reperfusion. FEBS J. *282*, 259–270.

Klein, I., Cornejo, J.C., Polakos, N.K., John, B., Wuensch, S.A., Topham, D.J., Pierce, R.H., and Crispe, I.N. (2007). Kupffer cell heterogeneity: functional properties of bone marrow derived and sessile hepatic macrophages. Blood *110*, 4077–4085.

Kuida, K., Lippke, J.A., Ku, G., Harding, M.W., Livingston, D.J., Su, M.S., and Flavell, R.A. (1995). Altered cytokine export and apoptosis in mice deficient in interleukin-1 beta converting enzyme. Science *267*, 2000–2003.

Labbé, K., and Saleh, M. (2008). Cell death in the host response to infection. Cell Death Differ. *15*, 1339–1349.

Latz, E., Xiao, T.S., and Stutz, A. (2013). Activation and regulation of the inflammasomes. Nat. Rev. Immunol. *13*, 397–411.

LeBlanc, P.M., Doggett, T.A., Choi, J., Hancock, M.A., Durocher, Y., Frank, F., Nagar, B., Ferguson, T.A., and Saleh, M. (2014). An immunogenic peptide in the A-box of HMGB1 protein reverses apoptosis-induced tolerance through RAGE receptor. J. Biol. Chem. *289*, 7777–7786.

Li, H., Fan, X., Stoicov, C., Liu, J.H., Zubair, S., Tsai, E., Ste Marie, R., Wang, T.C., Lyle, S., Kurt-Jones, E., and Houghton, J. (2009). Human and mouse colon cancer utilizes CD95 signaling for local growth and metastatic spread to liver. Gastroenterology *137*, 934–944, 944.e1–944.e4.

Lodolce, J.P., Boone, D.L., Chai, S., Swain, R.E., Dassopoulos, T., Trettin, S., and Ma, A. (1998). IL-15 receptor maintains lymphoid homeostasis by supporting lymphocyte homing and proliferation. Immunity *9*, 669–676.

Manfredi, S., Lepage, C., Hatem, C., Coatmeur, O., Faivre, J., and Bouvier, A.M. (2006). Epidemiology and management of liver metastases from colorectal cancer. Ann. Surg. *244*, 254–259.

Martinon, F., Mayor, A., and Tschopp, J. (2009). The inflammasomes: guardians of the body. Annu. Rev. Immunol. *27*, 229–265.

Novick, D., Kim, S., Kaplanski, G., and Dinarello, C.A. (2013). Interleukin-18, more than a Th1 cytokine. Semin. Immunol. *25*, 439–448.

Okamoto, M., Liu, W., Luo, Y., Tanaka, A., Cai, X., Norris, D.A., Dinarello, C.A., and Fujita, M. (2010). Constitutively active inflammasome in human melanoma cells mediating autoinflammation via caspase-1 processing and secretion of interleukin-1beta. J. Biol. Chem. *285*, 6477–6488.

Okamura, H., Tsutsi, H., Komatsu, T., Yutsudo, M., Hakura, A., Tanimoto, T., Torigoe, K., Okura, T., Nukada, Y., Hattori, K., et al. (1995). Cloning of a new cytokine that induces IFN-gamma production by T cells. Nature *378*, 88–91.

Qin, Y., Ekmekcioglu, S., Liu, P., Duncan, L.M., Lizée, G., Poindexter, N., and Grimm, E.A. (2011). Constitutive aberrant endogenous interleukin-1 facilitates inflammation and growth in human melanoma. Mol. Cancer Res. *9*, 1537–1550.

Rosenberg, S.A., Spiess, P., and Lafreniere, R. (1986). A new approach to the adoptive immunotherapy of cancer with tumor-infiltrating lymphocytes. Science *233*, 1318–1321.

Salcedo, R., Worschech, A., Cardone, M., Jones, Y., Gyulai, Z., Dai, R.M., Wang, E., Ma, W., Haines, D., O'hUigin, C., et al. (2010). MyD88-mediated signaling prevents development of adenocarcinomas of the colon: role of interleukin 18. J. Exp. Med. *207*, 1625–1636.

Schreiber, R.D., Old, L.J., and Smyth, M.J. (2011). Cancer immunoediting: integrating immunity's roles in cancer suppression and promotion. Science *331*, 1565–1570.

Shao, W., Yeretssian, G., Doiron, K., Hussain, S.N., and Saleh, M. (2007). The caspase-1 digestome identifies the glycolysis pathway as a target during infection and septic shock. J. Biol. Chem. *282*, 36321–36329.

Shi, Y., Evans, J.E., and Rock, K.L. (2003). Molecular identification of a danger signal that alerts the immune system to dying cells. Nature *425*, 516–521.

Smyth, M.J., Swann, J., Kelly, J.M., Cretney, E., Yokoyama, W.M., Diefenbach, A., Sayers, T.J., and Hayakawa, Y. (2004). NKG2D recognition and perforin effector function mediate effective cytokine immunotherapy of cancer. J. Exp. Med. *200*, 1325–1335.

Terme, M., Ullrich, E., Aymeric, L., Meinhardt, K., Desbois, M., Delahaye, N., Viaud, S., Ryffel, B., Yagita, H., Kaplanski, G., et al. (2011). IL-18 induces PD-1-dependent immunosuppression in cancer. Cancer Res. *71*, 5393–5399.

Terme, M., Ullrich, E., Aymeric, L., Meinhardt, K., Coudert, J.D., Desbois, M., Ghiringhelli, F., Viaud, S., Ryffel, B., Yagita, H., et al. (2012). Cancer-induced immunosuppression: IL-18-elicited immunoablative NK cells. Cancer Res. *72*, 2757–2767.

Tsikitis, V.L., Larson, D.W., Huebner, M., Lohse, C.M., and Thompson, P.A. (2014). Predictors of recurrence free survival for patients with stage II and III colon cancer. BMC Cancer *14*, 336.

Tu, S., Bhagat, G., Cui, G., Takaishi, S., Kurt-Jones, E.A., Rickman, B., Betz, K.S., Penz-Oesterreicher, M., Bjorkdahl, O., Fox, J.G., and Wang, T.C. (2008). Overexpression of interleukin-1beta induces gastric inflammation and cancer and mobilizes myeloid-derived suppressor cells in mice. Cancer Cell *14*, 408–419.

Valcárcel, M., Carrascal, T., Crende, O., and Vidal-Vanaclocha, F. (2014). IL-18 regulates melanoma VLA-4 integrin activation through a hierarchized sequence of inflammatory factors. J. Invest. Dermatol. *134*, 470–480.

Viaud, S., Saccheri, F., Mignot, G., Yamazaki, T., Daillère, R., Hannani, D., Enot, D.P., Pfirschke, C., Engblom, C., Pittet, M.J., et al. (2013). The intestinal microbiota modulates the anticancer immune effects of cyclophosphamide. Science *342*, 971–976.

Wallin, R.P., Screpanti, V., Michaëlsson, J., Grandien, A., and Ljunggren, H.G. (2003). Regulation of perforin-independent NK cell-mediated cytotoxicity. Eur. J. Immunol. *33*, 2727–2735.

Zaki, M.H., Boyd, K.L., Vogel, P., Kastan, M.B., Lamkanfi, M., and Kanneganti, T.D. (2010a). The NLRP3 inflammasome protects against loss of epithelial integrity and mortality during experimental colitis. Immunity *32*, 379–391.

Zaki, M.H., Vogel, P., Body-Malapel, M., Lamkanfi, M., and Kanneganti, T.D. (2010b). IL-18 production downstream of the Nlrp3 inflammasome confers protection against colorectal tumor formation. J. Immunol. *185*, 4912–4920.

Zheng, H.X., Cai, Y.D., Wang, Y.D., Cui, X.B., Xie, T.T., Li, W.J., Peng, L., Zhang, Y., Wang, Z.Q., Wang, J., and Jiang, B. (2013). Fas signaling promotes motility and metastasis through epithelial-mesenchymal transition in gastrointestinal cancer. Oncogene *32*, 1183–1192.